Supporting Information

Integrating β-ketoenamine Linkage into Covalent Organic Frameworks toward Efficient Overall Photocatalytic Hydrogen Peroxide Production

Chang Shu[#,1], Peixuan Xie[#,1], Xiaoju Yang[1], Xuan Yang[1], Hui Gao[1], Bien Tan[1,*], Xiaoyan Wang[1,*]

Table of Contents

1. Supplemental experimental procedures

1.1 chemicals

Mesitylene, 1,4-Dioxane, N,N-Dimethylacetamide were obtained from Innochem. 4,4',4''-(1,3,5-Triazine-2,4,6-triyl)trianiline (Tz), 2-Hydroxy-1,3,5-benzenetricarboxaldehyde (HBZ), 2,4-Dihydroxy-1,3,5-benzenetricarboxaldehyde (DHBZ), 1,3,5-Triformylphloroglucinol (THBZ) were obtained from Shanghai Tensus Bio-tech Co., Ltd. All chemicals were used as received and without further purification.

1.2 Synthesis procedures

Synthesis of Tz-HBZ: A Pyrex tube (10 mL) was charged with 4,4',4''-(1,3,5-Triazine-2,4,6-triyl)trianiline (53 mg, 0.15 mmol) and 2-Hydroxy-1,3,5-benzenetricarboxaldehyde (26 mg, 0.15 mmol), mesitylene (1.5 mL), 1,4-dioxane (1.5 mL) and aqueous acetic acid (0.5 mL, 6 M). The mixture was ultrasonicated for two minutes and then flash frozen at 77 K (liquid N_2 bath) and degassed through three freeze-pump-thaw cycles and sealed under vacuum using a Schlenk line and oil pump. The tube was heated at 120°C for 5 days. After cooling to room temperature, the precipitate was washed with DMF and then the solvent was exchanged with acetone 6 times. The powder was collected and dried at 120°C under vacuum overnight. Anal. Calcd for $(C_{30}H_{18}N_6O)_n$: C, 75.31; H, 3.77; N, 17.57. Found: C, 58.54; H, 5.48; N, 14.47.

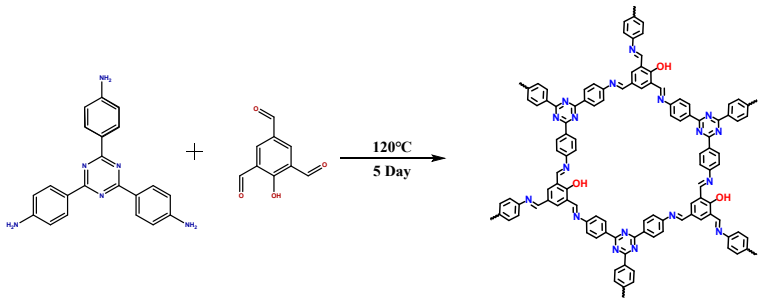

Figure S1. Scheme of the synthesis of Tz-HBZ.

Synthesis of Tz-DHBZ: A Pyrex tube (10 mL) was charged with 4,4',4''-(1,3,5-Triazine-2,4,6-triyl)trianiline (53 mg, 0.15 mmol) and 2-Hydroxy-1,3,5-benzenetricarboxaldehyde (30 mg, 0.15 mmol), N,N-Dimethylacetamide (1.5 mL), 1,4-dioxane (0.75 mL) and aqueous acetic acid (0.25 mL, 6 M). The mixture was ultrasonicated for two minutes and then flash frozen at 77 K (liquid N_2 bath) and degassed through three freeze-pump-thaw cycles and sealed

under vacuum using a Schlenk line and oil pump. The tube was heated at 120°C for 5 days. After cooling to room temperature, the precipitate was washed with DMF and then the solvent was exchanged with acetone 6 times. The powder was collected and dried at 120°C under vacuum overnight. Anal. Calcd for $(C_{30}H_{18}N_6O_2)_n$: C, 70.59; H, 3.53; N, 16.47. Found: C, 51.67; H, 5.91; N, 12.22.

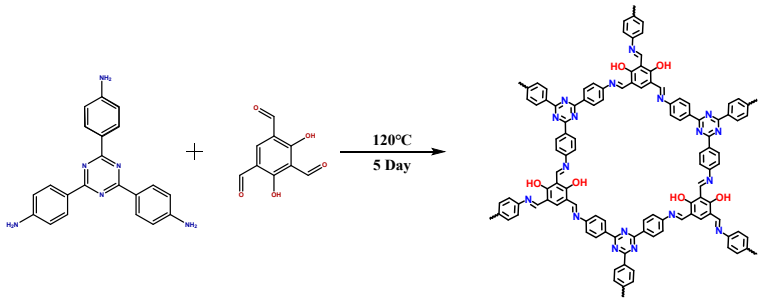

Figure S2. Scheme of the synthesis of Tz-DHBZ.

Synthesis of Tz-THBZ: A Pyrex tube (10 mL) was charged with 4,4',4''-(1,3,5-Triazine-2,4,6-triyl)trianiline (53 mg, 0.15 mmol) and 1,3,5-Triformylphloroglucinol (33 mg, 0.15 mmol), mesitylene (1.5 mL), 1,4-dioxane (1.5 mL) and aqueous acetic acid (0.5 mL, 6 M). The mixture was ultrasonicated for two minutes and then flash frozen at 77 K (liquid N_2 bath) and degassed through three freeze-pump-thaw cycles and sealed under vacuum using a Schlenk line and oil pump. The tube was heated at 120°C for 5 days. After cooling to room temperature, the precipitate was washed with DMF and then the solvent was exchanged with acetone 6 times. The powder was collected and dried at 120°C under vacuum overnight. Anal. Calcd for $(C_{30}H_{18}N_6O_3)_n$: C, 68.44; H, 3.42; N, 15.97. Found: C, 59.78; H, 5.48; N, 14.47.

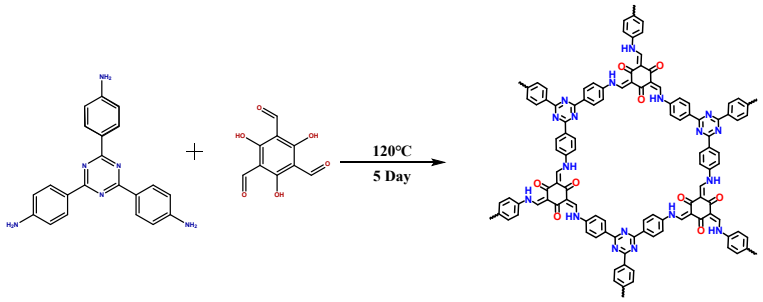

Figure S3. Scheme of the synthesis of Tz-THBZ.

2. Characterization methods

Fourier transform infrared (FT-IR) spectra were measured in transmission on a Tensor 27 FT-IR spectrometer (Bruker) using KBr pellets at room temperature. The thermal properties of the polymer networks were performed using a differential thermal analysis instrument (Q1000DSC + LNCS + FACS Q600SDT) over the temperature range from 30 to 800°C under a nitrogen atmosphere with a heating rate of 10°C min^{-1}. Element analysis was obtained by an EURO EA3000 Element Analyzer. The water contact angle was carried out by a video optical contact angle tester (Dataphysics-OCA20). Solid-state ^{13}C-NMR spectra were recorded on a JEOL RESONANCE ECZ 400R NMR spectrometer at a MAS rate of 12 kHz. Powder X-ray diffraction measurements (PXRD) were carried out on an X-ray Diffractometer (D/Max-3c). The morphology analysis was carried out using a field emission scanning electron microscope (SEM) (JSM-6700F) and high-resolution transmission electron microscopy (HR-TEM) (TECNAI G2 F30S). The UV-Vis absorption spectra of the COFs were obtained on a Scan UV-Vis spectrophotometer (UV-Lambda 950, PerkinElmer, US). Surface areas and pore size distributions were measured by nitrogen adsorption and desorption at 77.3 K using an ASAP 2420-4 (Micromeritics) volumetric adsorption analyzer. Time-correlated single photon counting (TCSPC) measurements were conducted using a single photon counting controller (Fluorohub, Horiba Scientific) to collect the photoluminescence decay profiles. Spin trapping electron paramagnetic resonance (EPR) measurement was performed by ESR spectrometer (Bruker, EMXmicro-6/1) and 5,5-dimethyl-1-pyrroline N-oxide (DMPO) was used as a spin-trapping reagent.

3. Photo-electrochemical analysis

Photocurrent measurement

A three-electrode cell was employed to measure the photocurrent on a CHI660E (Chenhua, Shanghai) electrochemical workstation. The working electrode was prepared by coating the mixture slurry of the polymer catalyst. 5% Nafion solution and ethanol as the binder on FTO, where the coating area was 1 cm^2. The working electrode was dried at 50°C for 0.5 hours before the measurement. A platinum plate and a saturated calomel electrode were used as the counter electrode and reference electrode, respectively and 0.5 M sodium sulfate solution was used as the electrolyte. A 300 W Xenon lamp was applied to illuminate the sample.

Electrochemical impedance measurement

A three-electrode cell was employed to measure the photocurrent and cyclic voltammetry on a CHI660E (Chenhua, Shanghai) electrochemical workstation. The working electrode, counter electrode and reference electrode are glassy carbon electrode, platinum plate and a saturated calomel electrode, respectively. The electrolyte was 0.5M sodium sulfate solution.

Mott-Schottky measurement

A three-electrode cell was employed to conduct the Mott-Schottky measurement on a CHI660E (Chenhua, Shanghai) electrochemical workstation. The working electrode was prepared by mixing ground polymer (2 mg) with isopropanol (0.3 mL) containing 5wt% Nafion and then was sonicated for 10 min. A 200 μL sample was taken and deposited on FTO with an area of 1 cm^2. A platinum plate and a saturated calomel electrode were employed as the counter electrode and reference electrode, respectively. The electrolyte was 0.2M sodium sulfate solution.

4. Photocatalytic experiments

The as-prepared COF photocatalyst (10 mg) was fully dispersed in deionized water (50 mL) by ultrasonicating for 10 min. Then, the mixture solution was removed to a reaction flask and illuminated by a 300 W Xenon lamp source (Microsolar 300) with a filter (λ > 420 nm) and stirred under an air atmosphere. Circulating cooling water was employed to keep the photocatalytic reaction temperature at 25°C. After the reaction, 1 mL solution was sampled with an injection syringe and then filtered with a 0.2 μm Millipore filter to remove the photocatalyst. The amount of H_2O_2 produced was analyzed by using the KI titrimetric method.

The external quantum efficiency (EQE) measurement for H_2O_2 evolution used 50 mg polymer in deionized water (50 mL) and was measured with monochromatic light obtained by using bandpass filters of 420, 450, 500, 550 and 600 nm, respectively. The irradiation area was controlled as 4×3.14 cm^2. EQE for H_2O_2 production at monochromatic light irradiation was estimated as below equation.

$$EQE(\%) = \frac{2 \times \text{Number of evolved } H_2O_2 \text{ molecules}}{\text{Number of incident photons}} = \frac{2 \times M \times N_A}{S \times P \times t \times \frac{\lambda}{h \times c}} \times 100\%$$

Where, M is the amount of hydrogen peroxide molecules (mol), N_A is Avogadro constant (6.022 × 10^{23} /mol), h is the Planck constant (6.626 × 10^{-34} J·s), *c* is

the speed of light (3×10^8 m/s), S is the irradiation area (cm^2), P is the intensity of irradiation light (W/cm^2), t is the photoreaction time (s), λ is the wavelength of the monochromatic light (m).

The solar-to-chemical energy conversion (SCC) efficiency measurement was conducted in a quartz vessel. The 50 mg catalyst was well dispersed in 50 mL deionized water and degassed by O_2 bubbling for 10 min before being sealed in a vessel. A Xenon solar simulator was used as the light source (AM 1.5G, 100 mW cm^{-2}). The reaction temperature was kept at 25°C. The SCC efficiency was calculated via the following equation:

$$\mathrm{SCC}\ (\%) = \frac{\left[\Delta G \text{ for } H_2O_2 \text{ generation } \left(\frac{J}{mol}\right)\right] \times \left[H_2O_2 \text{ produced (mol)}\right]}{\left[\text{total input energy (W)}\right] \times \left[\text{reaction times (s)}\right]} \times 100$$

Where, the free energy (ΔG) for H_2O_2 formation is 117 kJ mol^{-1}, the irradiance of the spectrum is 1000 W m^{-2} and the irradiated area is 3.14×10^{-4} m^2.

5. The theoretical reaction pathway of H_2O_2 generation

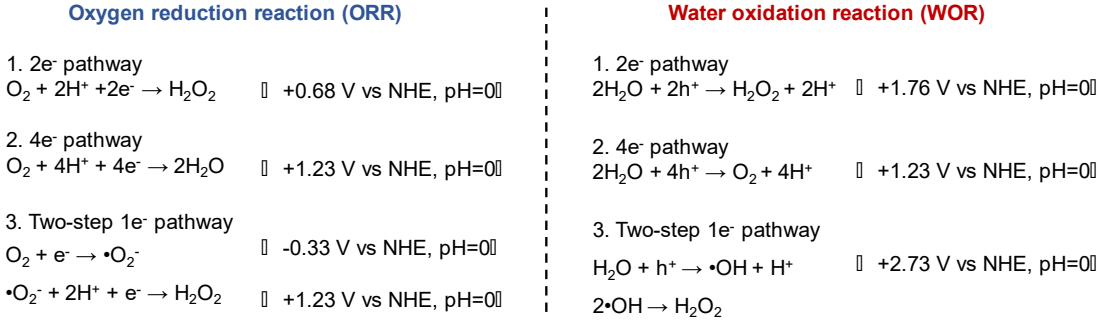

Figure S4. Energy diagrams for ORR and WOR pathways.

5. Supporting data

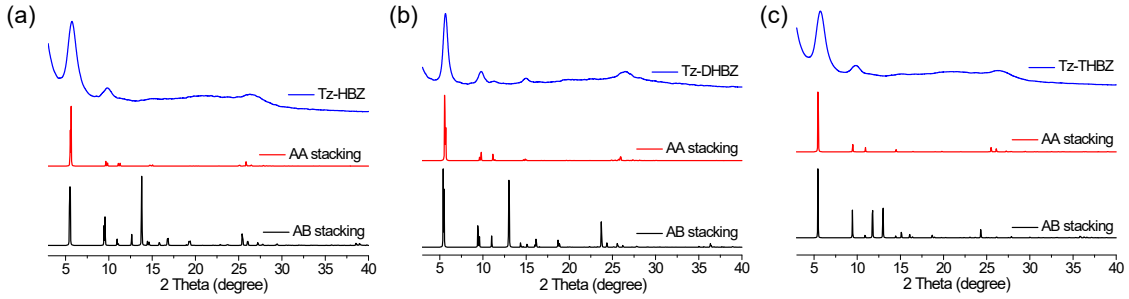

Figure S5. PXRD patterns of experimental (blue) and simulated (red and black) (a) Tz-HBZ, (b) Tz-DHBZ and (c) Tz-THBZ.

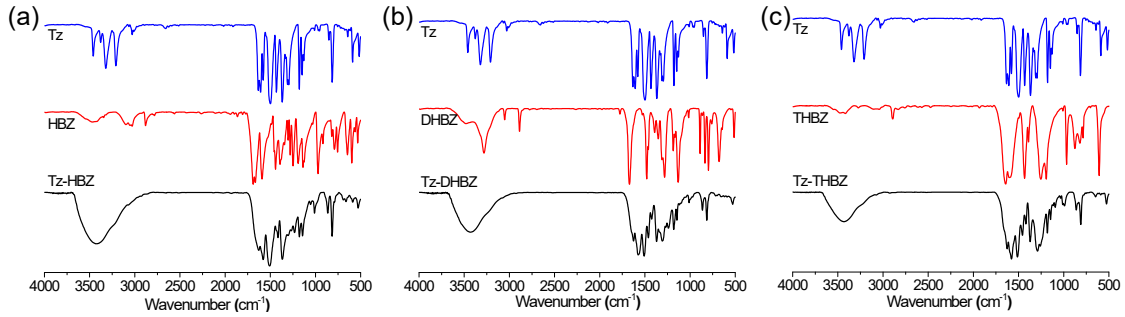

Figure S6. Transmission FT-IR spectra of the COFs and reactant monomers (a) Tz-HBZ, (b) Tz-DHBZ and (c) Tz-THBZ.

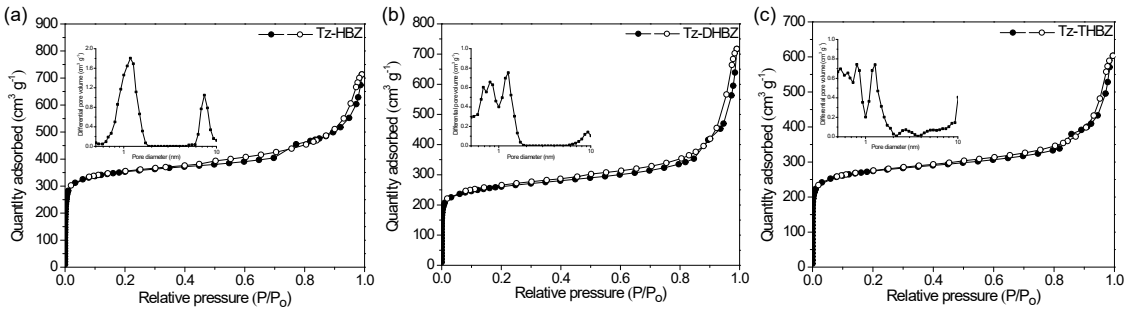

Figure S7. Nitrogen adsorption (filled symbols) and desorption (open symbols) isotherms were recorded at 77.3 K. The inset shows the calculated pore size distribution. (a) Tz-HBZ, (b) Tz-DHBZ and (c)Tz-THBZ.

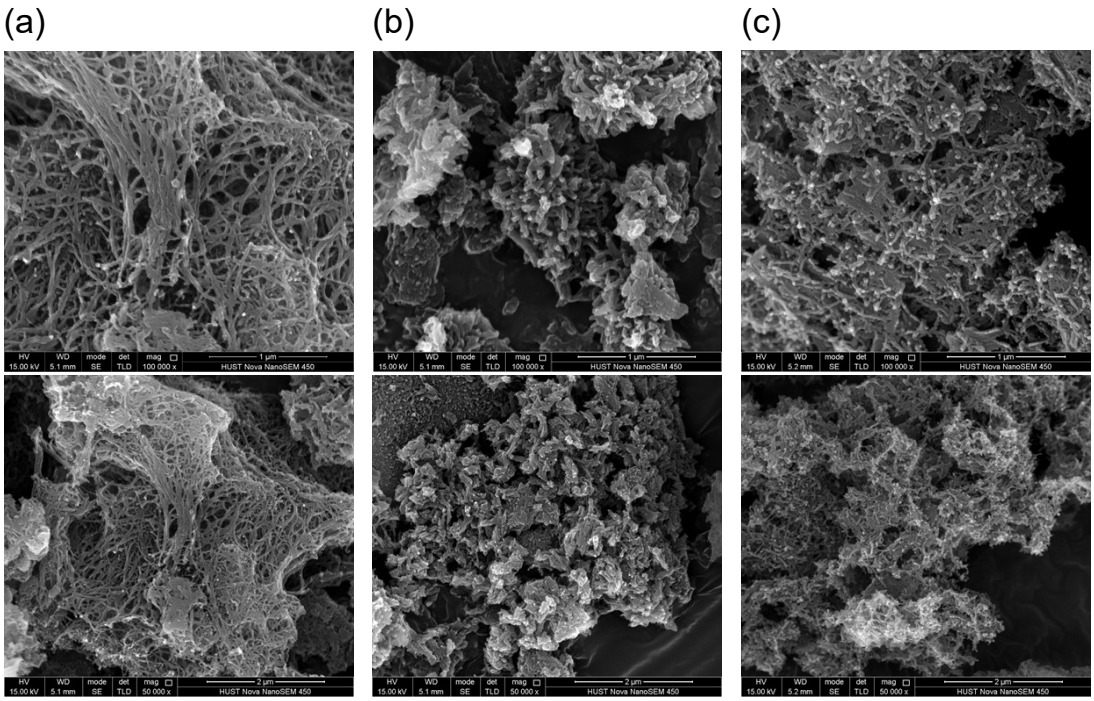

Figure S8. SEM images of the COFs: (a) Tz-HBZ, (b) Tz-DHBZ and (c) Tz-THBZ.

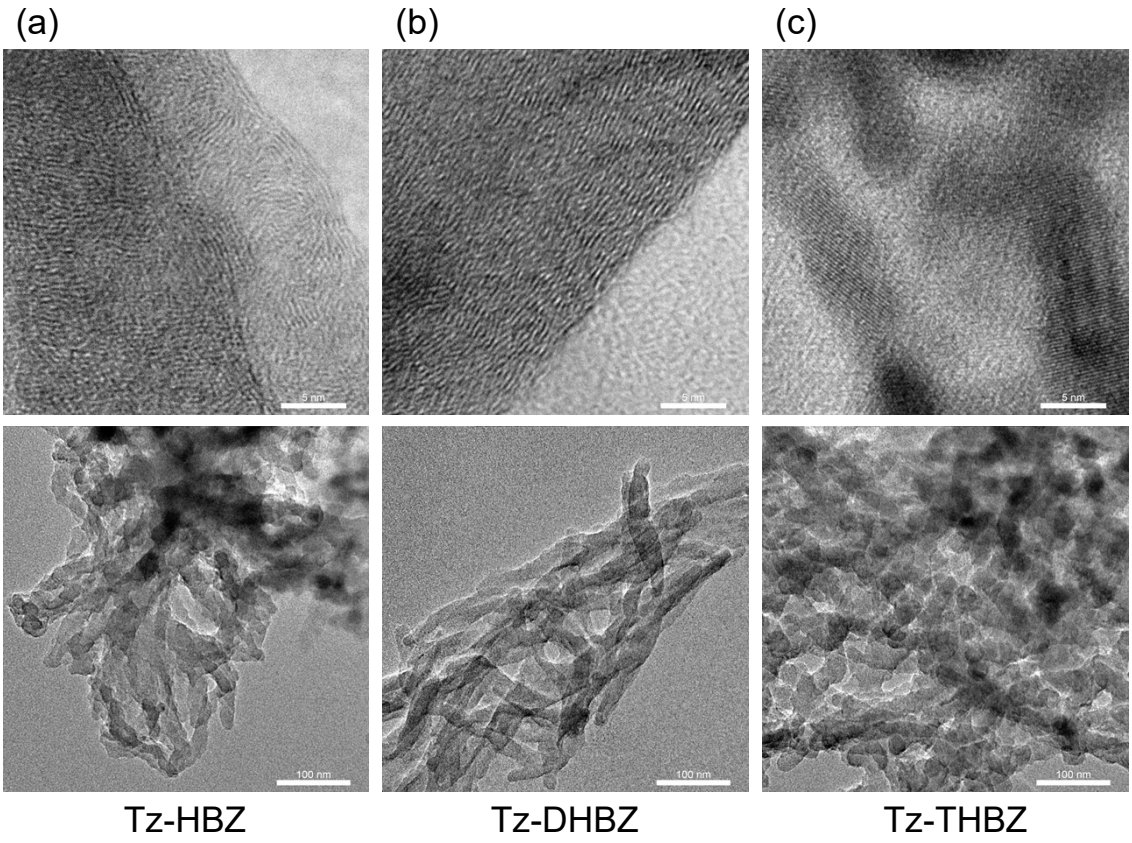

Figure S9. TEM images of the COFs: (a) Tz-HBZ, (b) Tz-DHBZ and (c) Tz-THBZ.

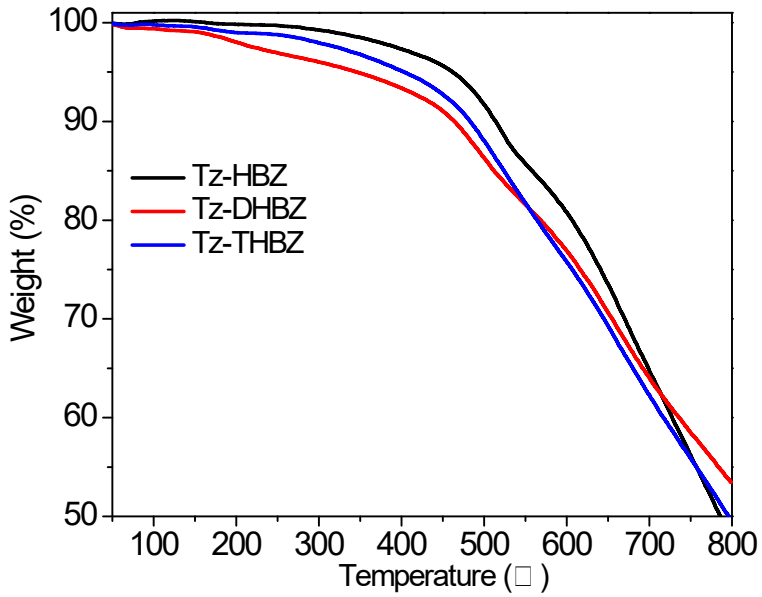

Figure S10. The thermogravimetric analysis traces the COFs under a nitrogen atmosphere.

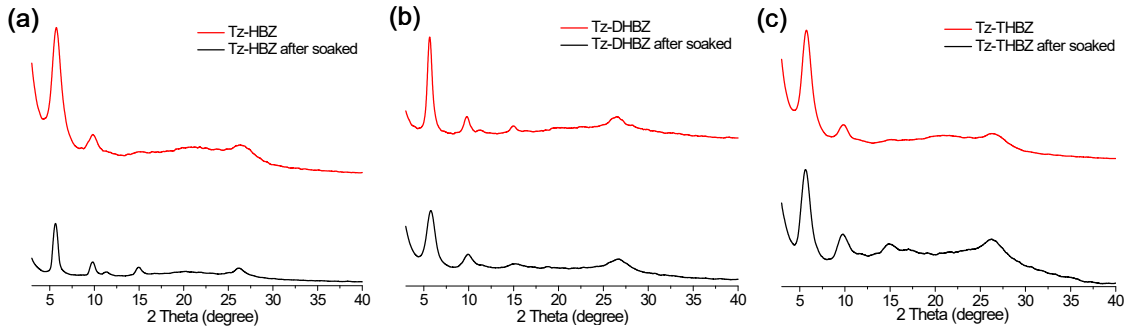

Figure S11. PXRD patterns of COFs after soaked in 1M concentration H_2O_2 for 48 hours. (a) Tz-HBZ, (b) Tz-DHBZ and (c)Tz-THBZ.

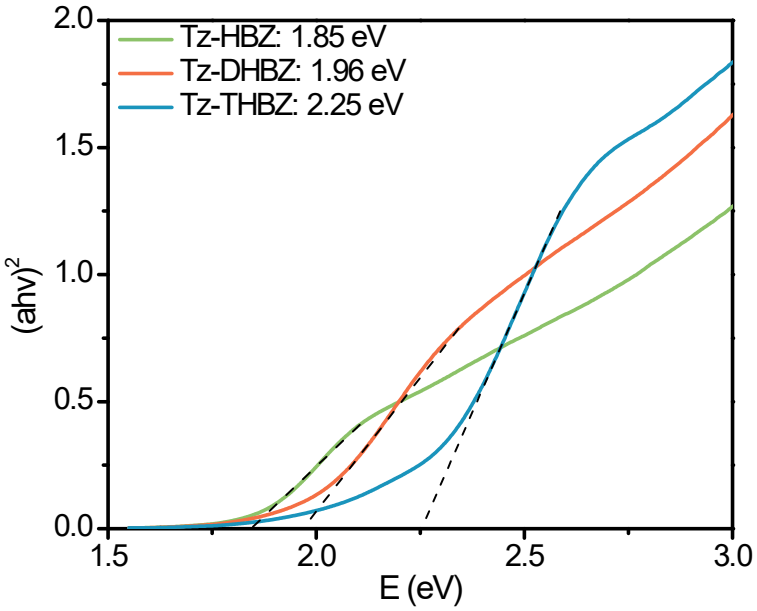

Figure S12. Tauc plots of the transformed Kubelka−Munk function *vs.* energy of the COFs.

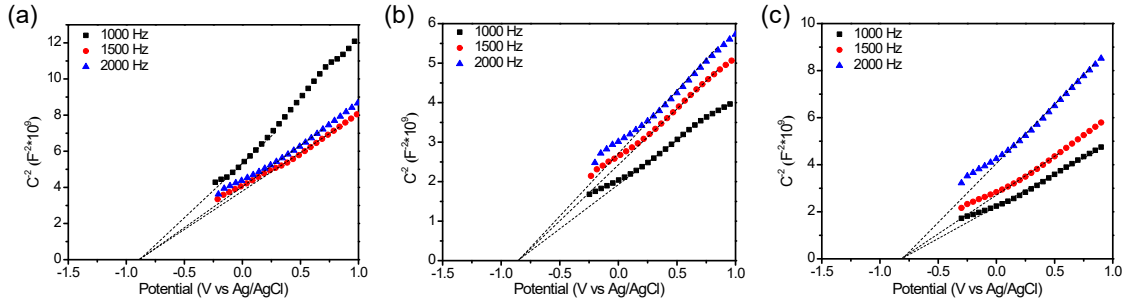

Figure S13. Mott−Schottky plot of the (a) Tz-HBZ, (b) Tz-DHBZ and (c)Tz-THBZ.

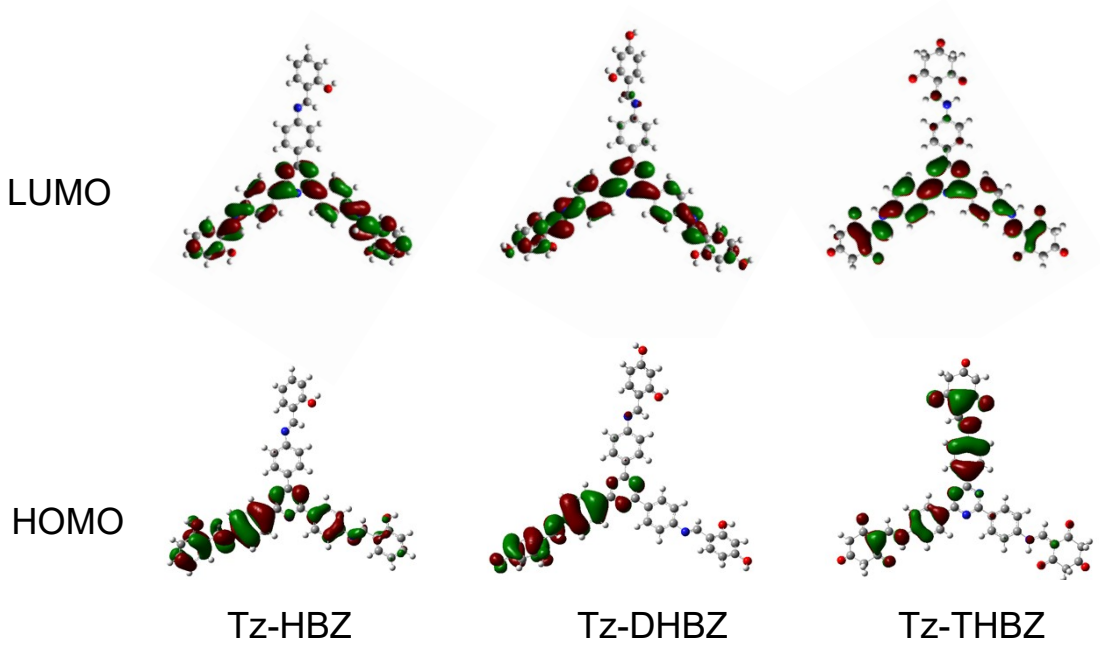

Figure S14. The HOMO and LUMO orbital distributions of the simplified Tz-HBZ, Tz-DHBZ and Tz-THBZ fragments from DFT simulation.

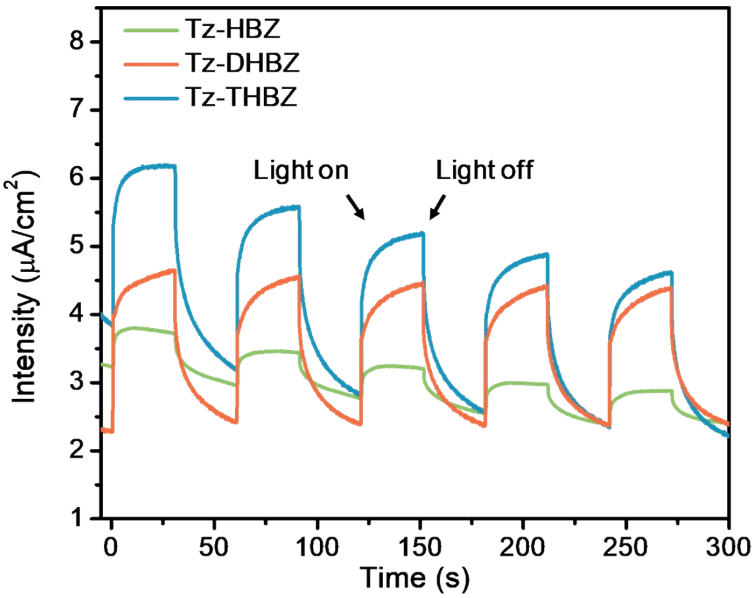

Figure S15. Transient photocurrent of the COFs.

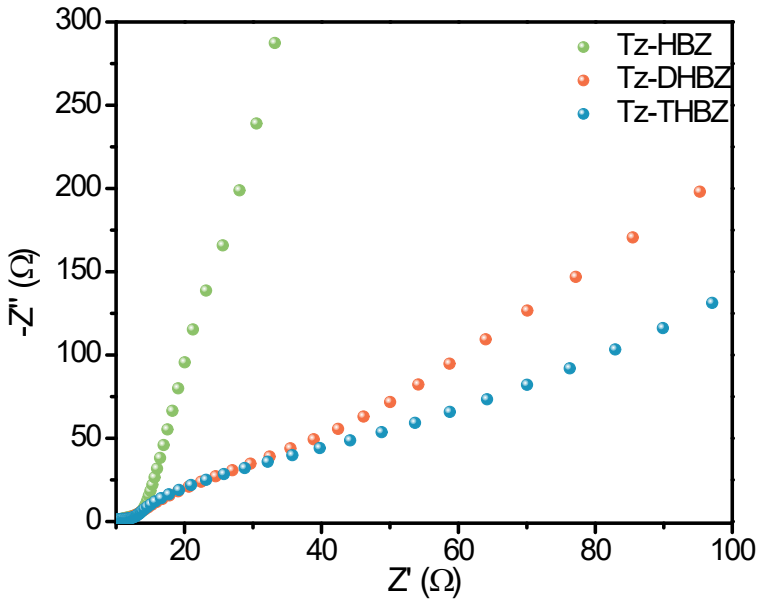

Figure S16. EIS spectra of the COFs.

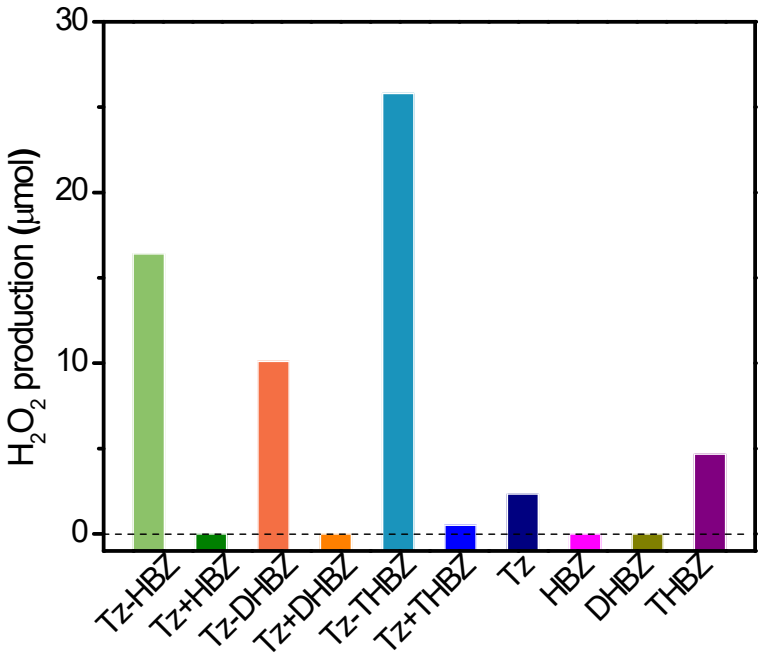

Figure S17. Photocatalytic reaction of COFs and physical mixtures of their ingredients (10 mg catalyst or monomer (the mass ratio of physical mixture is 1:1) in 50 mL water under visible light (λ > 420 nm) for 1 hour)).

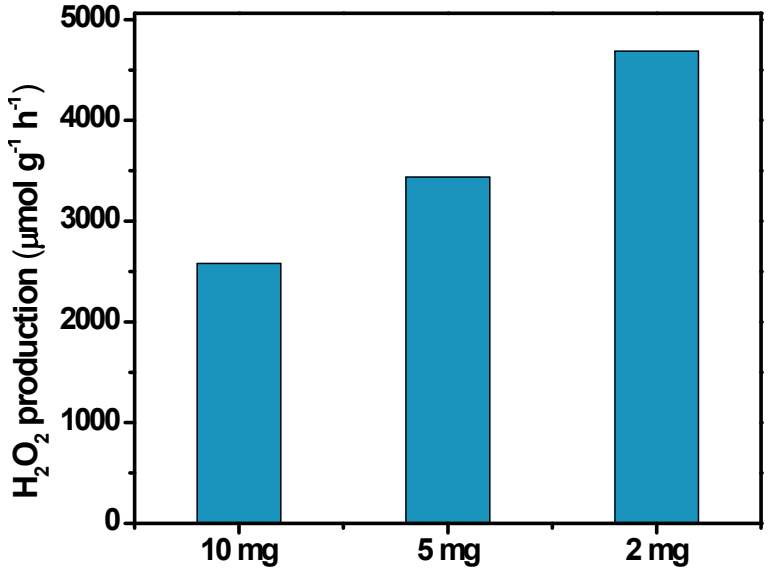

Figure S18. Photocatalytic activity of Tz-THBZ with different amounts of catalyst in 50 mL water under visible light (λ > 420 nm) for 1 hour.

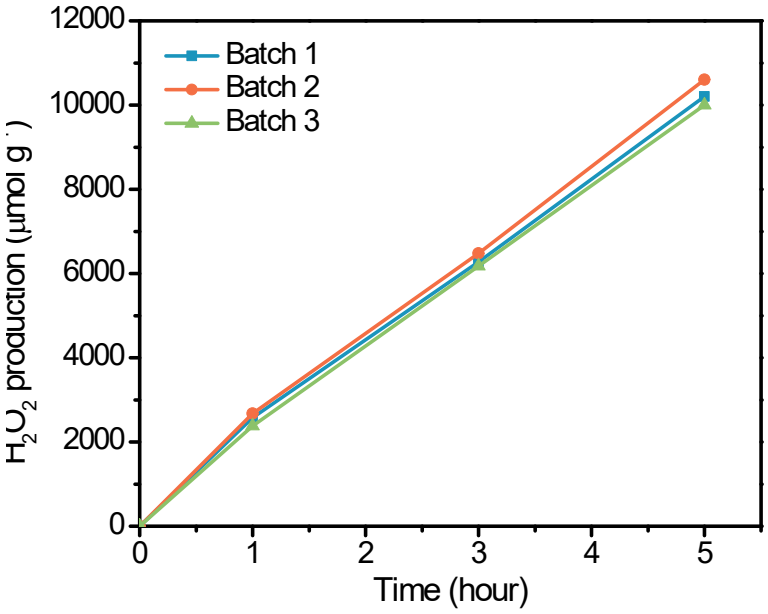

Figure S19. Photocatalytic activity of Tz-THBZ produced from three different batches (10 mg catalyst in 50 mL water under visible light (λ > 420 nm)).

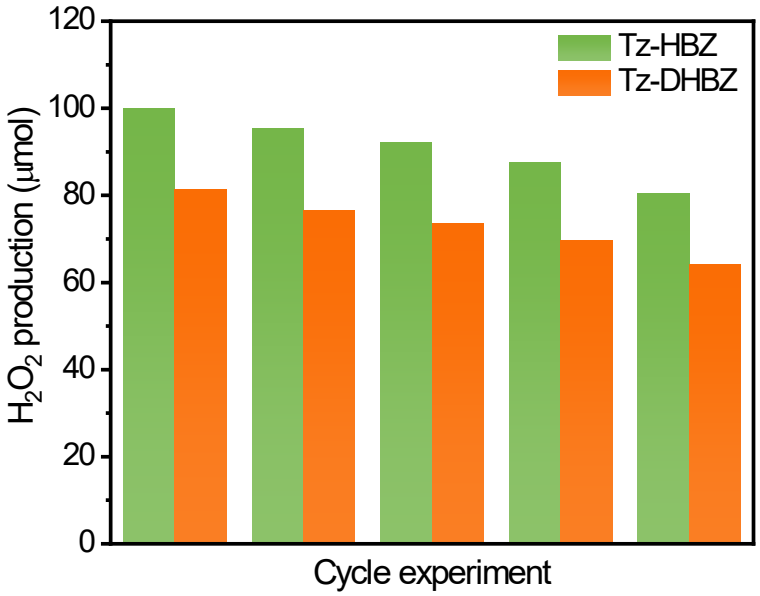

Figure S20. Photocatalytic cycle performance of Tz-HBZ and Tz-DHBZ (50 mg catalyst in 50 mL water under visible light, λ > 420 nm, 10 hours for each cycle).

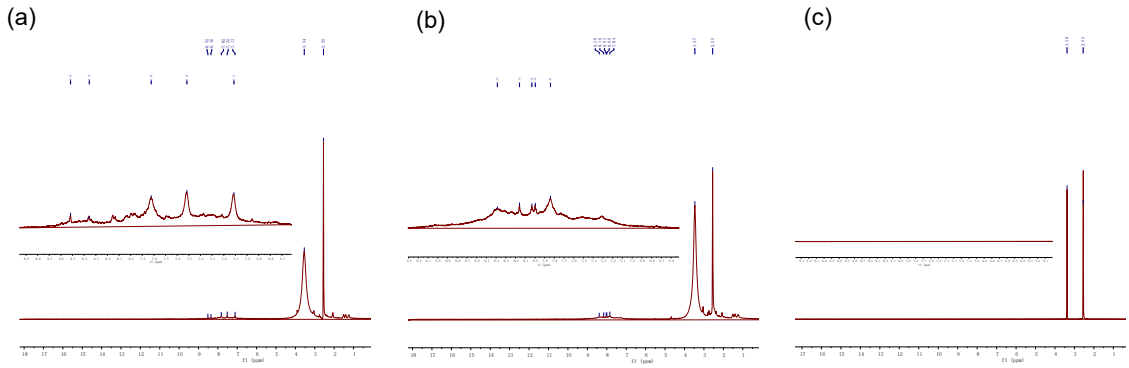

Figure S21. ^{1}H-NMR of filtered photocatalytic reaction solution of COF in DMSO-d_6 after cycle experiment. (a) Tz-HBZ, (b) Tz-DHBZ and (c) Tz-THBZ.

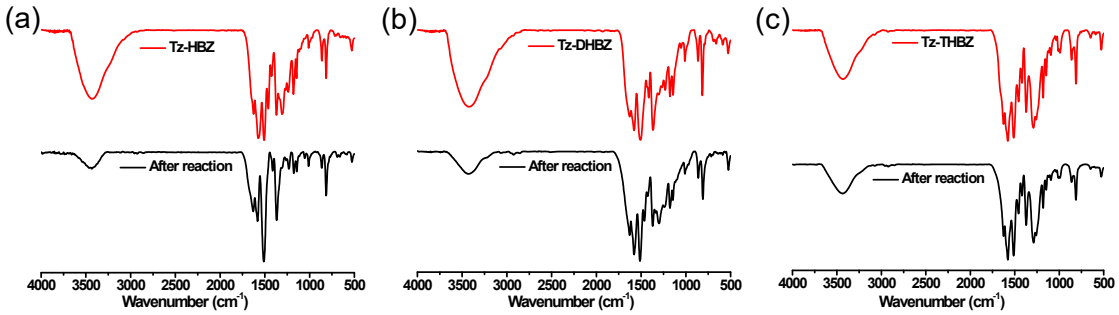

Figure S22. FT-IR spectra of COF after cycle experiment. (a) Tz-HBZ, (b) Tz-DHBZ and (c) Tz-THBZ

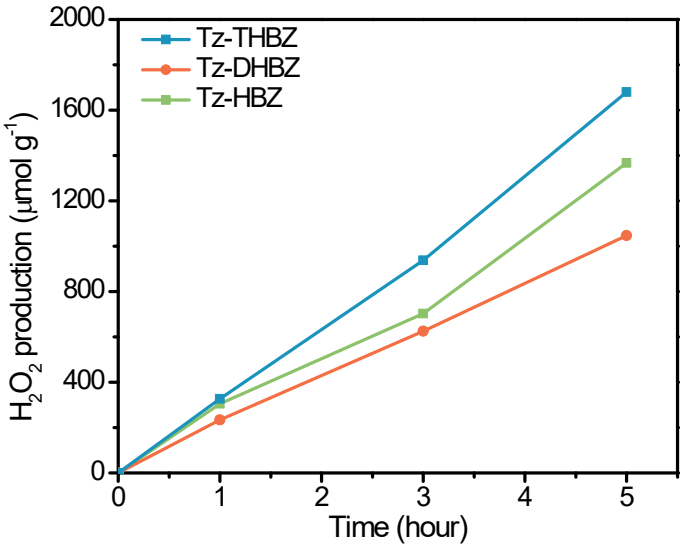

Figure S23. Photocatalytic H_2O_2 production performances for Tz-HBZ, Tz-DHBZ and Tz-THBZ (10 mg catalyst in 50 mL water at N_2 atmosphere under visible light (λ > 420 nm)).

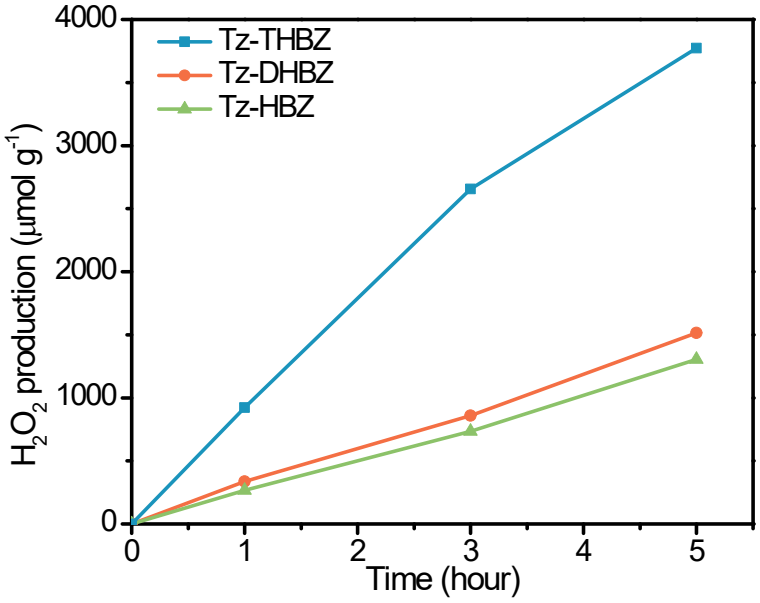

Figure S24. Photocatalytic H_2O_2 production performances for Tz-HBZ, Tz-DHBZ and Tz-THBZ (10 mg catalyst in 50 mL 1mM $KBrO_3$ solution at N_2 atmosphere under visible light (λ > 420 nm)).

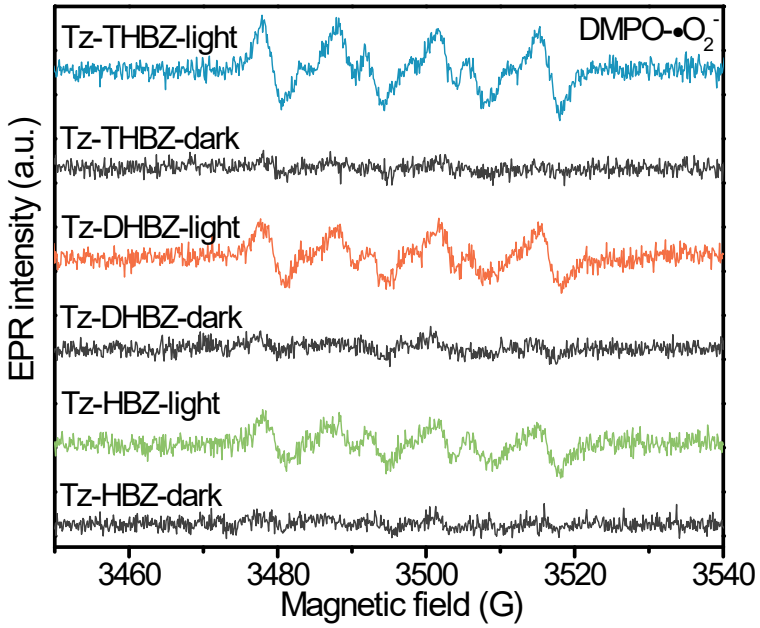

Figure S25. EPR experiments for Tz-THBZ using DMPO as the electron-trapping agent.

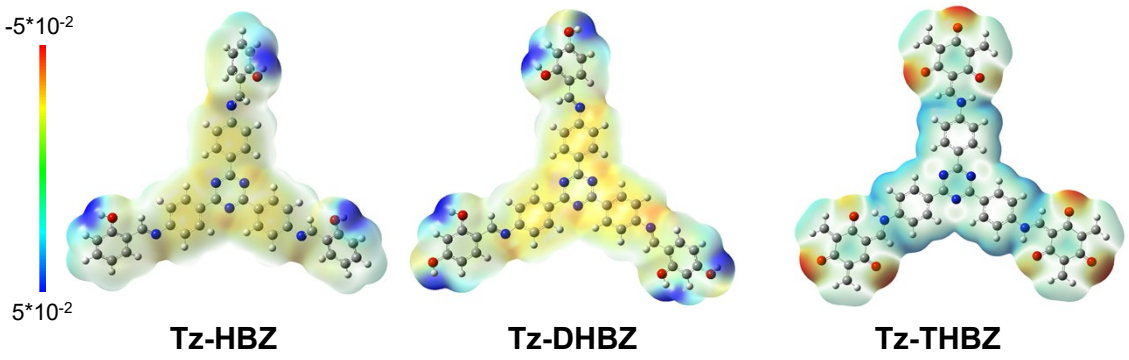

Figure S26. Electrostatic surface potential maps of COFs.

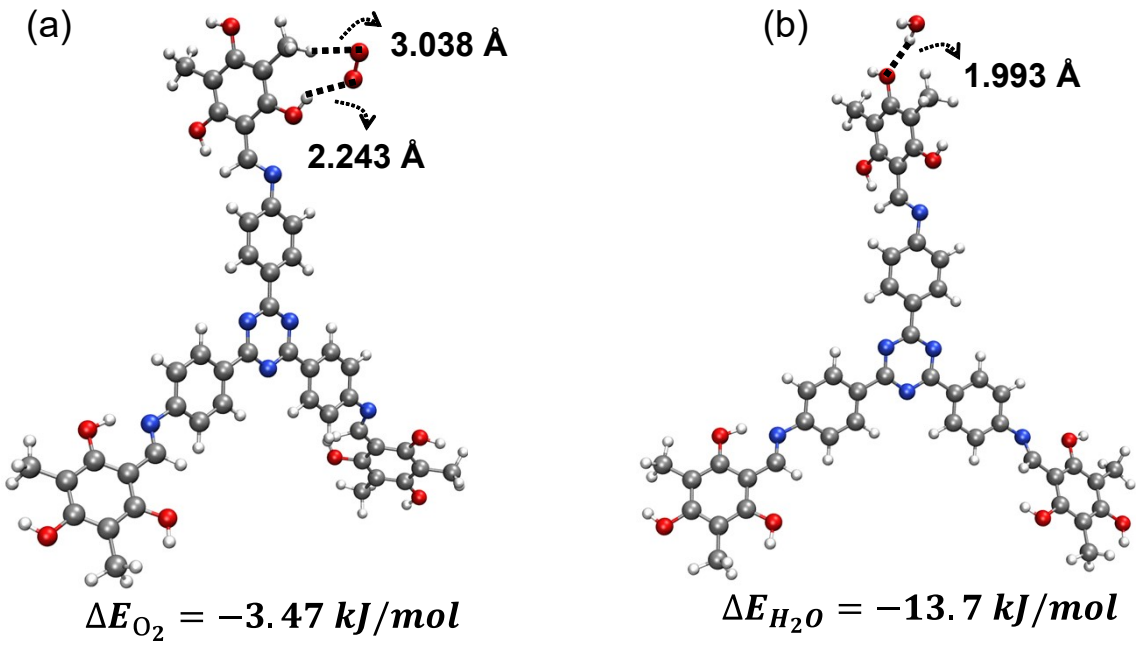

Figure S27. DFT-calculated adsorption configuration of (a) O_2 and (b) H_2O on enol-formed Tz-THBZ.

6. Supporting table

Table S1. Summary of the photocatalytic hydrogen peroxide production performance of various reported organic photocatalysts.

Photocatalyst	λ (nm)	Dosage (g/L)	Reaction solution*	H_2O_2 production (μM/h)	Stability (hour)	EQE (%)	SCC (%)	Ref.
Tz-THBZ	≥420	1	H_2O		6 cycles for 60 h	5.5@400 nm	0.36	This work
CHF-DPDA	≥420	2	water	3450	3 cycles for 18 h	16.0@420 nm	0.78	[1]
COF-N32	≥420	0.5	water	302.5	12 h	6.2@459 nm	0.31	[2]
SO_3H-COF	≥400	0.1	water	301.5	5 cycles for 4.17 h	8.7@400 nm	0.41	[3]
DE7-M	≥420	1.7	water	2444	5 cycles for 10 h	8.70@420 nm	0.23	[4]

COF-TfpBpy	≥420	0.5	water	1042	5 cycles for 40 h	8.10@420 nm	0.57	[5]
Nv–C≡N–CN	≥420	1	water	137	5 cycles for 5 h	3.10@400 nm	0.23	[6]
PAF-363	420	1	water	78.6	12 h	5.3@420 nm	-	[7]
TAPD-$(Me)_2$	≥420	4	H_2O:EtOH (9:1)	316	5 cycles for 10 h	--	--	[8]
DCNS	≥400	1	H_2O:EtOH (9:1)	3080	4 cycles for 12 h	6.80@400 nm	--	[9]
TPB-DMTP-COF	≥420	0.2	water	330	5 cycles for 5 h	18.4@420 nm	0.76	[10]
DVA-COF	420	0.5	H_2O:BA (9:1)	4225	16 h	2.84@420 nm	0.08	[11]
g-C_3N_4/PDI_{51}	≥420	1.7	water	34.6	--	2.60@420 nm	--	[12]
5Cv@g-C_3N_4	≥420	1	H_2O:EtOH (9:1)	7010	5 cycles for 5 h	14.3@365 nm	--	[13]
RF/P_3HT	≥300	1.7	water	1013.1	10 cycles for 10 h	10.5@420 nm	1.00	[14]
TF_{50}-COF	≥400	0.1	H_2O:EtOH (9:1)	172	--	5.10@400 nm	0.17	[15]
Bpt-CTF	-	0.2	water	654	10 cycles for 10 h	8.60@400 nm	0.20	[16]
TBTN-COF	420	0.125	water	1376.6	5 cycles for 5 h	7.6@420 nm	-	[17]
Py-Da-COF	≥420	1	water	461	4 cycles for 8 h	2.40@420 nm	0.09	[18]
4PE-N-S	≥420	0.25	water	393.5	5 cycles for 5 h	--	--	[19]
CoPc-BTM-COF	≥400	0.1	H_2O:EtOH (9:1)	209.6	4 cycles for 4 h	7.20@630 nm	--	[20]
NMT400	AM 1.5G	0.4	H_2O:EtOH (9:1)	678	6 cycles for 6 h	0.50@475 nm	--	[21]
PMCR-1	≥420	0.45	water	656.8	--	14.0@420 nm	--	[22]
P-TAME	≥420	1	PB:H_2O (2:9)	13500	5 cycles for 20 h	--	--	[23]
COF-TTA-TTTA	≥420	0.3	water	721.8	6 cycles for 24 h	--	--	[24]
PEI/C_3N_4	AM 1.5G	1	water	208.1	3 cycles for 3 h	2.12@420 nm	0.045	[25]
CN4	≥420	0.5	H_2O:IPA (9:1)	28.7	3 cycles for 3 h	27.8@420 nm	--	[26]
TB-COF	≥400	0.125	water	706.5	5 cycles for 5 h	3.45@420 nm	1.08	[27]
FS-COFs	≥400	0.25	water	375.4	4 cycles for 8 h	6.21@420 nm	--	[28]
TpDz	≥420	0.167	water	1221	4 cycles for 4 h	11.9@420 nm	0.62	[29]

* EtOH: ethanol; IPA: isopropanol; BA: benzyl alcohol; PB: phenylcarbinol; TEOA: triethanolamine.

7. Computational details

All DFT calculations were performed using the CP2K code.[30] The calculations utilized mixed Gaussian and plane wave basis sets. Core electrons were described using norm-conserving Goedecker-Teter-Hutter pseudopotentials,[31-33] while the valence electron wavefunction was expanded in a double-zeta basis set with polarization functions,[34] supplemented by an auxiliary plane wave basis set with an energy cutoff of 400 eV. The Perdew, Burke, and Enzerhof (PBE)[35] generalized gradient approximation exchange-correlation functional was applied. Each configuration was optimized using the Broyden-Fletcher-Goldfarb-Shanno (BGFS) algorithm with SCF convergence criteria set at 1.0×10^{-6} au. To include the long-range van der Waals dispersion interaction, the DFT-D3 scheme[36] with an empirical damped potential term was incorporated into the energies calculated from the exchange-correlation functional in all simulations.

The adsorption energy between the COF and the H_2O/O_2 adsorbates can be calculated using the following equation:

$$\Delta E = E_{adsorbate/COF} - E_{COF} - E_{adsorbate} \quad \text{(S1)}$$

In Eq. (S1), $E_{adsorbate/COF}$ and E_{COF} represent the total energies of the COF with and without the adsorption of the adsorbates, respectively. $E_{adsorbate}$ is the total energy of the H_2O or O_2 adsorbates.

8. References

1. H. Cheng, H. Lv, J. Cheng, L. Wang, X. Wu and H. Xu, *Adv. Mater.*, 2022, **34**, 2107480.

2. F. Liu, P. Zhou, Y. Hou, H. Tan, Y. Liang, J. Liang, Q. Zhang, S. Guo, M. Tong and J. Ni, *Nat. Commun.*, 2023, **14**, 4344.

3. L. Li, X. Lv, Y. Xue, H. Shao, G. Zheng and Q. Han, *Angew. Chem. Int. Ed.*, 2024, **63**, e202320218.

4. L. Liu, M.-Y. Gao, H. Yang, X. Wang, X. Li and A. I. Cooper, *J. Am. Chem. Soc.*, 2021, **143**, 19287-19293.

5. M. Kou, Y. Wang, Y. Xu, L. Ye, Y. Huang, B. Jia, H. Li, J. Ren, Y. Deng, J. Chen, Y. Zhou, K. Lei, L. Wang, W. Liu, H. Huang and T. Ma, *Angew. Chem. Int. Ed.*, 2022, **61**, e202200413.

6. X. Zhang, P. Ma, C. Wang, L. Gan, X. Chen, P. Zhang, Y. Wang, H. Li, L. Wang, X. Zhou and K. Zheng, *Energ. Environ. Sci.*, 2022, **15**, 830-842.

7. L. Cao, C. Wang, H. Wang, X. Xu, X. Tao, H. Tan and G. Zhu, *Angew. Chem. Int. Ed.*, 2024**, 63**, e202402095.

8. C. Krishnaraj, H. Sekhar Jena, L. Bourda, A. Laemont, P. Pachfule, J. Roeser, C. V. Chandran, S. Borgmans, S. M. J. Rogge, K. Leus, C. V. Stevens, J. A. Martens, V. Van Speybroeck, E. Breynaert, A. Thomas and P. Van Der Voort, *J. Am. Chem. Soc.*, 2020, **142**, 20107-20116.

9. Q. He, B. Viengkeo, X. Zhao, Z. Qin, J. Zhang, X. Yu, Y. Hu, W. Huang and Y. Li, *Nano Res.* 2023, **16**, 4524-4530.

10. L. Li, L. Xu, Z. Hu and J. C. Yu, *Adv. Funct. Mater.*, 2021, **31**, 2106120.

11. H. Yu, F. Zhang, Q. Chen, P.-K. Zhou, W. Xing, S. Wang, G. Zhang, Y. Jiang and X. Chen, *Angew. Chem. Int. Ed.*, 2024**, 63**, e202402297.

12. Y. Shiraishi, S. Kanazawa, Y. Kofuji, H. Sakamoto, S. Ichikawa, S. Tanaka and T. Hirai, *Angew. Chem. Int. Ed.*, 2014, **53**, 13454-13459.

13. L. Chen, C. Chen, Z. Yang, S. Li, C. Chu and B. Chen, *Adv. Funct. Mater.*, 2021, **31**, 2105731.

14. Y. Shiraishi, M. Matsumoto, S. Ichikawa, S. Tanaka and T. Hirai, *J. Am. Chem. Soc.*, 2021, **143**, 12590-12599.

15. H. Wang, C. Yang, F. Chen, G. Zheng and Q. Han, *Angew. Chem. Int. Ed.*, 2022, **61**, e202202328.

16. C. Wu, Z. Teng, C. Yang, F. Chen, H. B. Yang, L. Wang, H. Xu, B. Liu, G. Zheng and Q. Han, *Adv. Mater.*, 2022*,* **34**, 2110266.

17. E. Zhou, F. Wang, Y. Hui and Y. Wang, *Angew. Chem. Int. Ed.*, 2024**,** **63**, e202400999.

18. J. Sun, H. Sekhar Jena, C. Krishnaraj, K. Singh Rawat, S. Abednatanzi, J. Chakraborty, A. Laemont, W. Liu, H. Chen, Y.-Y. Liu, K. Leus, H. Vrielinck, V. Van Speybroeck and P. Van Der Voort, *Angew. Chem. Int. Ed.*, 2023, **62**, e202216719.

19. M. Deng, J. Sun, A. Laemont, C. Liu, L. Wang, L. Bourda, J. Chakraborty, K. Van Hecke, R. Morent, N. De Geyter, K. Leus, H. Chen and P. Van Der Voort, *Green Chem.*, 2023, **25**, 3069-3076.

20. Q. Zhi, W. Liu, R. Jiang, X. Zhan, Y. Jin, X. Chen, X. Yang, K. Wang, W. Cao, D. Qi and J. Jiang, *J. Am. Chem. Soc.*, 2022, **144**, 21328-21336.

21. C. Yang, S. Wan, B. Zhu, J. Yu and S. Cao, *Angew. Chem. Int. Ed.*, 2022, **61**, e202208438.

22. P. Das, J. Roeser and A. Thomas, *Angew. Chem. Int. Ed.*, 2023, **62**, e202304349.

23. Z. Luo, X. Chen, Y. Hu, X. Chen, W. Lin, X. Wu and X. Wang, *Angew. Chem. Int. Ed.*, 2023, **62**, e202304875.

24. F. Tan, Y. Zheng, Z. Zhou, H. Wang, X. Dong, J. Yang, Z. Ou, H. Qi, W. Liu, Z. Zheng and X. Chen, *CCS Chem.*, 2022, **4**, 3751-3761.

25. X. Zeng, Y. Liu, Y. Kang, Q. Li, Y. Xia, Y. Zhu, H. Hou, M. H. Uddin, T. R. Gengenbach, D. Xia, C. Sun, D. T. McCarthy, A. Deletic, J. Yu and X. Zhang, *ACS Catal.*, 2020, **10**, 3697-3706.

26. C. Feng, L. Tang, Y. Deng, J. Wang, J. Luo, Y. Liu, X. Ouyang, H. Yang, J. Yu and J. Wang, *Adv. Funct. Mater.*, 2020, **30**, 2001922.

27. J.-Y. Yue, L.-P. Song, Z.-X. Pan, P. Yang, Y. Ma, Q. Xu and B. Tang, *ACS Catalysis*, 2024, **14**, 4728-4737.

28. Y. Luo, B. Zhang, C. Liu, D. Xia, X. Ou, Y. Cai, Y. Zhou, J. Jiang and B. Han, *Angew. Chem. Int. Ed.*, 2023, **62**, e202305355.

29. Q. Liao, Q. Sun, H. Xu, Y. Wang, Y. Xu, Z. Li, J. Hu, D. Wang, H. Li and K. Xi, *Angew. Chem. Int. Ed.*, 2023, **62**, e202310556.

30. J. VandeVondele, M. Krack, F. Mohamed, M. Parrinello, T. Chassaing and J. Hutter, *Comput. Phys. Commun.*, 2005, **167**, 103-128.

31. S. Goedecker, M. Teter and J. Hutter, *Phys. Rev. B*, 1996, **54**, 1703-1710.

32. C. Hartwigsen, S. Goedecker and J. Hutter, *Phys. Rev. B*, 1998, **58**, 3641-3662.

33. M. Krack and M. Parrinello, *Phys. Chem. Chem. Phys.*, 2000, **2**, 2105-2112.

34. J. VandeVondele and J. Hutter, *J. Chem. Phys.*, 2007, **127**, 114105.

35. J. P. Perdew, K. Burke and M. Ernzerhof, *Phys. Rev. Lett.*, 1996, **77**, 3865.

36. S. Grimme, J. Antony, S. Ehrlich and H. Krieg, *J. Chem. Phys.*, 2010, **132**, 154104.